

Stiffened orthotropic corner supported hypar shells: Effect of stiffener location, rise/span ratio and fiber orientation on vibration behavior

Kutlu Darilmaz

*Department of Civil Engineering
Istanbul Technical University 34469, Maslak, Istanbul, Turkey*

(Received December 08, 2011, Revised January 10, 2012, Accepted January 17, 2012)

Abstract. In this paper the influence of stiffener location, rise/span ratio and fibre orientation on vibration behavior of corner supported hypar shells is studied by using a four-node hybrid stress finite element. The formulation of the element is based on Hellinger-Reissner variational principle. The element is developed by combining a hybrid plane stress element and a hybrid plate element. Benchmark problems are solved to validate the approach and free vibration response of stiffened orthotropic hypar shells is studied both with respect to fundamental frequency and mode shapes by varying the location of stiffeners, rise/span ratio and fiber orientation.

Keywords: stiffened hypar shell, assumed stress hybrid element, finite element, free vibration

1. Introduction

Hypar shell structures have been widely used as roofing members since they can be cast and fabricated conveniently being doubly ruled surfaces. In some cases hypar shells may be stiffened to have enhanced rigidity. The vibration behavior of such and similar structures have been analysed by various researchers. Schwarte (1994) examined the natural frequencies and mode shapes of isotropic and linear elastic shallow hyperbolic paraboloidal shells of rhombic planform with free edges and corner point supports, Sinha and Mukhopadhyay (1994) reported frequencies and mode shapes of stiffened isotropic cylindrical panels using finite element method. Sahoo and Chakravorty (2005), (2006), (2008) studied the behavior of stiffened hypar shell roofs and hypar shallow shells with various edge supports by using an eight noded shell element. Civalek (2007) presented a computational approach, the discrete singular convolution (DSC) algorithm, for the free vibration analysis of conical shells, Nanda and Bandyopadhyay (2008) compared their results of static and dynamic analyses of plates, cylindrical and spherical shells employing four-, eight-, and nine-noded elements with different integration rules with those of earlier investigators and including some of the recent composite theories. Haldar (2008) presented a composite triangular shallow shell element and used for free vibration analysis of laminated composite skewed cylindrical shell panels. Das and Chakravorty (2010) applied a

* Corresponding author, Ph.D., E-mail: darilmazk@itu.edu.tr

finite element code to study the bending behaviour of point supported composite shells. Dogan *et al.* (2010) studied effects of anisotropy and curvature on free vibration characteristics of cross-ply laminated composite shallow shells. Han *et al.* (2011) presented an improved 8-node shell element for the analysis of plates and shells based on a refined first-order shear deformation theory which is improved by the combined use of assumed natural strain method. Wang and Redekop (2011) studied the free vibration analysis of moderately-thick and thick toroidal shells based on a shear deformation (Timoshenko-Mindlin) shell theory.

In this paper, a flat shell element which is a combination of membrane element and a plate element is developed, based on the classical hybrid stress method which was first developed by Pian (1964). The element is generated by a combination of a hybrid plane stress element with drilling d.o.f. and a hybrid plate element presented by the author in a previous study, Darilmaz (2005). By using this element influence of stiffener location, rise/span ratio and fibre orientation on vibration behavior of orthotropic hypar shells is studied.

2. Element stiffness formulation

The assumed-stress hybrid method is based on the independent prescriptions of stresses within the element and displacements on the element boundary. The element stiffness matrix is obtained using Hellinger-Reissner variational principle. The Hellinger-Reissner functional of linear elasticity allows displacements and stresses to be varied separately. This establishes the master fields. Two slave strain fields appear, one coming from displacements and one from stresses.

The Hellinger-Reissner functional can be written as

$$\Pi_{RH} = \int_V \{\sigma\}^T [D] \{u\} dV - \frac{1}{2} \int_V \{\sigma\}^T [S] \{\sigma\} dV \quad (1)$$

where $\{\sigma\}$ is the stress vector, $[S]$ is the compliance matrix relating strains, $\{\varepsilon\}$, to stress ($\{\varepsilon\} = [S]\{\sigma\}$), $[D]$ is the differential operator matrix corresponding to the linear strain-displacement relations ($\{\varepsilon\} = [D]\{u\}$) and V is the volume of structure.

The approximation for stresses and displacements can now be incorporated in the functional. The stress field is described in the interior of the element as

$$\{\sigma\} = [P]\{\beta\} \quad (2)$$

and a compatible displacement field is described by

$$\{u\} = [N]\{q\} \quad (3)$$

where $[P]$ and $[N]$ are matrices of stress and displacement interpolation functions, respectively, and $\{\beta\}$ and $\{q\}$ are the unknown stress and nodal displacement parameters, respectively. Intra-element equilibrating stresses and compatible displacements are independently interpolated. Since stresses are independent from element to element, the stress parameters are eliminated at the element level and a conventional stiffness matrix results. This leaves only the nodal displacement parameters to be assembled into the global system of equations.

Substituting the stress and displacement approximations Eq. (2), Eq. (3) in the functional Eq.(1)

yields

$$\Pi_{RH} = [\beta]^T [G] [q] - \frac{1}{2} [\beta]^T [H] [\beta] \quad (4)$$

where

$$[H] = \int_V [P]^T [S] [P] dV \quad (5)$$

$$[G] = \int_V [P]^T ([D] [N]) dV \quad (6)$$

Now imposing stationary conditions on the functional with respect to the stress parameters $\{\beta\}$ gives

$$[\beta] = [H]^{-1} [G] [q] \quad (7)$$

Substitution of $\{\beta\}$ in Eq. (4), the functional reduces to

$$\Pi_{RH} = \frac{1}{2} [q]^T [G]^T [H]^{-1} [G] [q] = \frac{1}{2} [q]^T [K] [q] \quad (8)$$

where

$$[K] = [G]^T [H]^{-1} [G] \quad (9)$$

is recognized as a stiffness matrix.

The solution of the system yields the unknown nodal displacements $\{q\}$. After $\{q\}$ is determined, element stresses or internal forces can be recovered by use of Eq. (7) and Eq. (2). Thus

$$\{\sigma\} = [P][H]^{-1}[G]\{q\} \quad (10)$$

3. Governing equations

Consider a hyper shell of uniform thickness which the orthotropic material property may be arbitrarily oriented at an angle ϕ with reference to the x-axis of the local coordinate system Fig. 1.

The stress-strain relation with respect to x, y and z axes can be written as

$$\begin{Bmatrix} \sigma_x \\ \sigma_y \\ \tau_{xy} \end{Bmatrix} = \begin{bmatrix} \bar{\Omega}_{11} & \bar{\Omega}_{12} & \bar{\Omega}_{16} \\ \bar{\Omega}_{12} & \bar{\Omega}_{22} & \bar{\Omega}_{26} \\ \bar{\Omega}_{16} & \bar{\Omega}_{26} & \bar{\Omega}_{66} \end{bmatrix} \begin{Bmatrix} \varepsilon_x \\ \varepsilon_y \\ \gamma_{xy} \end{Bmatrix} \text{ or } \{\sigma\} = [\bar{\Omega}_{ij}]\{\varepsilon\} \quad (i,j=1,2,6) \quad (11)$$

$$\begin{Bmatrix} \tau_{xz} \\ \tau_{yz} \end{Bmatrix} = \begin{bmatrix} \bar{\Omega}_{44} & \bar{\Omega}_{45} \\ \bar{\Omega}_{45} & \bar{\Omega}_{55} \end{bmatrix} \begin{Bmatrix} \gamma_{xz} \\ \gamma_{yz} \end{Bmatrix} \text{ or } \{\tau\} = [\bar{\Omega}_{ij}]\{\gamma\} \quad (i,j=4,5) \quad (12)$$

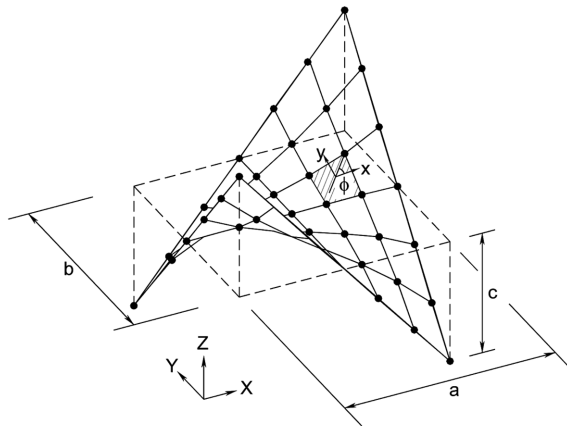


Fig. 1 Global and local axis of hypar shell

$[\bar{\Omega}_{ij}]$ in Eqs. (11) and (12) is defined as

$$[\bar{\Omega}_{ij}] = [T_1]^{-1} [\Omega_{ij}] [T_1]^{-T} \quad (i,j=1,2,6) \quad (13)$$

$$[\bar{\Omega}_{ij}] = [T_2]^{-1} [\Omega_{ij}] [T_2] \quad (i,j=4,5) \quad (14)$$

in which

$$[T_1] = \begin{bmatrix} \cos^2\phi & \sin^2\phi & 2\sin\phi\cos\phi \\ \sin^2\phi & \cos^2\phi & -2\sin\phi\cos\phi \\ -\sin\phi\cos\phi & \sin\phi\cos\phi & \cos^2\phi - \sin^2\phi \end{bmatrix} \quad (15)$$

$$[T_2] = \begin{bmatrix} \cos\phi & -\sin\phi \\ \sin\phi & \cos\phi \end{bmatrix} \quad (16)$$

$$[\Omega_{ij}] = \begin{bmatrix} \Omega_{11} & \Omega_{12} & 0 \\ \Omega_{12} & \Omega_{22} & 0 \\ 0 & 0 & \Omega_{66} \end{bmatrix} \quad (i,j=1,2,6), \quad [\Omega_{ij}] = \begin{bmatrix} \Omega_{44} & 0 \\ 0 & \Omega_{55} \end{bmatrix} \quad (i,j=4,5) \quad (17)$$

$$\Omega_{11} = \frac{E_1}{1 - v_{12}v_{21}} \quad \Omega_{12} = \frac{v_{12}E_2}{1 - v_{12}v_{21}} \quad \Omega_{22} = \frac{E_2}{1 - v_{12}v_{21}} \quad (18a)$$

$$\Omega_{66} = G_{12} \quad \Omega_{44} = G_{13} \quad \Omega_{55} = G_{23} \quad (18b)$$

$$G_{ij} = \frac{\sqrt{E_i E_j}}{2(1 + \sqrt{v_{ij} v_{ji}})} \quad (i,j=1,2,3) \quad (18c)$$

The stress resultants are given by

$$\begin{bmatrix} N_x & M_x \\ N_y & M_y \\ N_{xy} & M_{xy} \end{bmatrix} = \int_{-h/2}^{h/2} \begin{bmatrix} \sigma_x \\ \sigma_y \\ \tau_{xy} \end{bmatrix} \begin{bmatrix} 1 & z \end{bmatrix} dz \quad (19a)$$

$$\begin{bmatrix} Q_x \\ Q_y \end{bmatrix} = \int_{-h/2}^{h/2} \begin{bmatrix} \tau_{xz} \\ \tau_{yz} \end{bmatrix} dz \quad (19b)$$

From Eqs. (19a) and (19b) the constitutive equations of the folded plate are obtained as

$$\{F\} = [E]\{\chi\} \quad (20)$$

where

$$\{F\} = \{N_x, N_y, N_{xy}, M_x, M_y, M_{xy}, Q_x, Q_y\} \quad (21)$$

$$\{\chi\} = \{\varepsilon_x, \varepsilon_y, \gamma_{xy}, \kappa_x, \kappa_y, \kappa_{xy}, \gamma_{xz}, \gamma_{yz}\} \quad (22)$$

The elasticity matrix can be expressed as

$$[E] = \begin{bmatrix} [A_{ij}] & [B_{ij}] & 0 \\ [B_{ij}] & [C_{ij}] & 0 \\ 0 & 0 & [D_{ij}] \end{bmatrix} \quad (23)$$

in which

$$[A_{ij}] = \int_{-h/2}^{h/2} [\bar{\Omega}_{ij}] dz, [B_{ij}] = \int_{-h/2}^{h/2} [\bar{\Omega}_{ij}] z dz, [C_{ij}] = \int_{-h/2}^{h/2} [\bar{\Omega}_{ij}] z^2 dz \quad (i,j = 1,2,6) \quad (24a)$$

$$[D_{ij}] = \int_{-h/2}^{h/2} [\bar{\Omega}_{ij}] dz \quad (i,j=4,5) \quad (24b)$$

4. The hybrid stress element

The proposed element is generated by a combination of a hybrid membrane element and a hybrid plate element.

4.1 Membrane component of the element with drilling degree of freedom

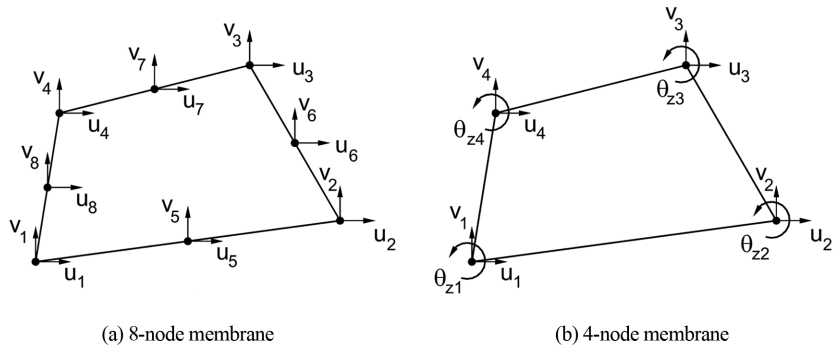


Fig. 2 Displacements for (a) 8-node membrane (b) 4-node membrane

Generally membrane elements have two translational d.o.f (u, v) per node but the need for membrane elements with a drilling degree of freedom arises in many engineering problems. A drilling rotation is defined as inplane rotation about the axis normal to the plane of element. This type of element is useful in solving folded plate structures and provides an easy coupling with edge beams which have six d.o.f per node. Inclusion of a drilling degree of freedom gives also the improved behavior of the element (Allman 1984, Choi and Lee 1996). The possibility of membrane elements with drilling d.o.f was opened by Allman (1984), Bergan and Felippa (1985). The concept has been further elaborated by many other researchers (Cook 1986, MacNeal and Harder 1988, Yunus *et al.* 1989, Ibrahimbegovic *et al.* 1990, Choi and Lee 1996) for more improved elements.

Formulation of drilling d.o.f for the present element is based on the procedure given by Yunus *et al.* (1989). The displacement fields are expressed in terms of translational and rotational d.o.f.'s at the corner nodes only.

The membrane displacement field for the 4-node element is derived from an 8-node element, Fig. 2. Rotational d.o.f. are associated with parabolic displaced shapes of element sides. In Fig. 3, rotational

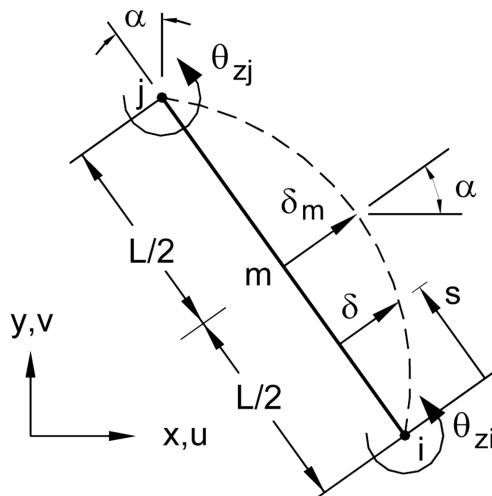


Fig. 3 Side displacement produced by drilling degrees of freedoms θ_{zi} and θ_{zj}

d.o.f. θ_{zi} and θ_{zj} are shown at nodes i and j of the element side of length L.

δ can be regarded as quadratic in side-tangent coordinates. θ_{zi} and θ_{zj} produce the edge normal displacement δ and midside value δ_m

$$\delta = \frac{s(L-s)}{2L}(\theta_{zi} - \theta_{zj}) \quad \delta_m = \frac{L}{8}(\theta_{zi} - \theta_{zj}) \quad (25)$$

The x and y components of δ are $\delta \cos\alpha$ and $\delta \sin\alpha$. Therefore, after adding the contribution to displacement from nodes i and j, the total displacements u and v of a typical point on the edge are

$$\begin{Bmatrix} u \\ v \end{Bmatrix} = \frac{L-s}{L} \begin{Bmatrix} u_i \\ v_i \end{Bmatrix} + \frac{s}{L} \begin{Bmatrix} u_j \\ v_j \end{Bmatrix} + \frac{(L-s)s}{2L} (\theta_{zj} - \theta_{zi}) \begin{Bmatrix} \cos\alpha \\ \sin\alpha \end{Bmatrix} \quad (26)$$

Side 1-5-2 of the element, Fig.2 d.o.f. at node 5 are related to d.o.f. at nodes 1 and 2 of the element. By evaluating Eq.2 with $s = L/2$ with $i = 1, j = 2$, $L\cos\alpha = y_2 - y_1$ and $L\sin\alpha = x_1 - x_2$, yields

$$\begin{Bmatrix} u_5 \\ v_5 \end{Bmatrix} = \frac{1}{2} \begin{Bmatrix} u_1 \\ v_1 \end{Bmatrix} + \frac{1}{2} \begin{Bmatrix} u_2 \\ v_2 \end{Bmatrix} + \frac{(\theta_{zi} - \theta_{zi})}{8} \begin{Bmatrix} y_2 - y_1 \\ x_1 - x_2 \end{Bmatrix} \quad (27)$$

After doing the same for d.o.f. at nodes 6, 7 and 8 d.o.f. in Fig. 1(b) and 1(c) by the transformation, the complete relation can be written

$$\{u_1 \quad v_1 \quad u_2 \quad v_2 \quad \dots \quad u_8 \quad v_8\}^T = [T]_{16 \times 12} \{q\}_{membrane}^T \quad (28)$$

where

$$\{q\}_{membrane} = \{u_1 \quad v_1 \quad \theta_{z1} \quad u_2 \quad v_2 \quad \theta_{z2} \quad u_3 \quad v_3 \quad \theta_{z3} \quad u_4 \quad v_4 \quad \theta_{z4}\} \quad (29)$$

So the midside nodal displacements can be written in terms of the corner nodal displacements and rotations and the displacement field for the 4-node, twelve d.o.f. membrane element can be derived from an 8-node membrane element. This is done through the use of the transformation matrix [T]. The form of [T] is given in Appendix 1.

The biggest difficulty in deriving hybrid finite elements seems to be the lack of a rational methodology for deriving stress terms , Feng *et al.* (1997), Darilmaz (2005). It is recognized that the number of stress modes m in the assumed stress field should satisfy

$$m \geq n - r \quad (30)$$

with n the total number of nodal displacements, and r the number of rigid body modes in an element. If Eq. (30) is not satisfied, use of too few coefficients in $\{\beta\}$, the rank of the element stiffness matrix will be less than the total degrees of deformation freedom and the numerical solution of the finite element model will not be stable and produces on element with one or more mechanism.

Increasing the number of β 's by adding stress modes of higher-order term, each extra term will add more stiffness and stiffens the element, Pian and Chen (1983), Punch and Atluri (1984).

The assumed stress field for the membrane part which satisfies the equilibrium conditions for zero body forces and avoid rank deficiency is given as

$$\begin{aligned} N_x &= \beta_1 + \beta_2 x + \beta_3 y + \beta_4 x^2 + \beta_5 xy + \beta_6 y^2 \\ N_y &= \beta_4 y^2 + \beta_7 + \beta_8 x + \beta_9 y + \beta_{10} x^2 + \beta_{11} xy \\ N_{xy} &= -\beta_2 y - 2\beta_4 xy - \beta_5 y^2 / 2 - \beta_9 x - \beta_{11} x^2 / 2 + \beta_{12} \end{aligned} \quad (31)$$

4.2 Plate component of the element

The flexural component of the element is identical to that of the plate bending element presented by the author, Darilmaz (2005), and corresponds to the Mindlin/Reissner plate theory. Only the assumed stress field which satisfies the equilibrium conditions for the plate part is given here.

$$\begin{aligned} M_x &= \beta_1 + \beta_4 y + \beta_6 x + \beta_8 xy \\ M_y &= \beta_2 + \beta_5 x + \beta_7 y + \beta_9 xy \\ M_{xy} &= \beta_3 + \beta_{10} x + \beta_{11} y + \beta_{12} x^2 / 2 + \beta_{13} y^2 / 2 \\ Q_x &= \beta_6 + \beta_{11} + \beta_8 y + \beta_{13} y \\ Q_y &= \beta_7 + \beta_{10} + \beta_9 x + \beta_{12} x \end{aligned} \quad (32)$$

The nodal displacements for the plate are chosen as

$$\{\mathbf{q}\}_{\text{plate}} = \{w_1 \quad \theta_{x1} \quad \theta_{y1} \quad w_2 \quad \theta_{x2} \quad \theta_{y2} \quad w_3 \quad \theta_{x3} \quad \theta_{y3} \quad w_4 \quad \theta_{x4} \quad \theta_{y4}\} \quad (33)$$

The combination of membrane and plate element yields the element which has 6 d.o.f per node and totally 24 d.o.f .

5. Element mass matrix

The problem of determination of the natural frequencies of vibration of a plate reduces to the solution of the standard eigenvalue problem $[K] - \omega^2 [M] = 0$, where ω is the natural circular frequency of the system. Making use of the conventional assemblage technique of the finite element method with the necessary boundary conditions, the system matrix $[K]$ and the mass matrix $[M]$ for the entire structure can be obtained.

Element mass matrix is derived from the kinetic energy expression

$$E_k = \frac{1}{2} \int_A \{\dot{\mathbf{q}}\}^T [R] \{\dot{\mathbf{q}}\} dA \quad (34)$$

where $\{\dot{\mathbf{q}}\}$ denotes the velocity components and $[R]$ is the inertia matrix.

The nodal and generalized velocity vectors are related with the help of shape functions

$$\{\dot{\mathbf{q}}\} = \sum_{i=1}^4 [N] \{\dot{q}_i\} \quad (35)$$

Substituting the velocity vectors in the kinetic energy, Eq.(34) yields the mass matrix of an element.

$$E_k = \frac{1}{2} \int_A \{\dot{q}_i\}^T [N]^T [R] [N] \{\dot{q}_i\} dA \quad (36)$$

$$E_k = \frac{1}{2} \int_A \{\dot{q}_i\}^T [m] \{\dot{q}_i\} dA \quad (37)$$

where $[m]$ is the element consistent mass matrix and is given by

$$[m] = \int_A [N]^T [R] [N] dA \quad (38)$$

6. Numerical examples

In order to validate the element behavior two comparative examples are solved. First a clamped square plate with one stiffener in one plan direction is analysed applying the present formulation making the rise of the hypar shell zero ($c=0$). A comparison of lowest fundamental frequency obtained by Mukherjee and Mukhopadhyay (1988), Nayak and Bandyopadhyay (2002), Sahoo and Chakravorty (2006) and this study is presented in Table 1. Higher frequencies are compared with ANSYS commercial finite element program.

Although the presented element shows a stiffer behaviour, the results are found to be in good agreement with previous works. A finer mesh is used for ANSYS solution for a better comparison result.

The first three mode shapes of the shell are depicted in Fig. 4.

Second validation example is the free vibration analysis of a corner point supported isotropic

Table 1. Natural frequencies (Hz) of centrally stiffened clamped square plate

Mode No	Present study (12×12)	ANSYS (Shell 63) (24×24 Mesh)	Mukherjee and Mukhopadhyay (1988)	Nayak and Bandyopadhyay (2002)	Sahoo and Chakravorty (2006)
1	750.62	754.36	711.8	725.1	733
2	755.37	756.51	---	---	---
3	991.36	995.73	---	---	---

$a = b = 0.2032$ m, shell thickness = 0.0013716 m, stiffener depth = 0.0127 m, stiffener width = 0.00635 m, Material property: $E = 6.87 \times 10^{10}$ N/m², $\nu = 0.29$, $\rho = 2823$ kg/m³.

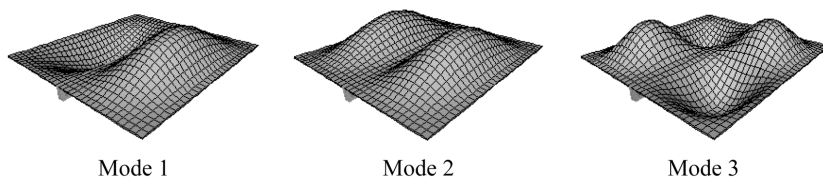


Fig. 4 First three modes of the stiffened clamped plate

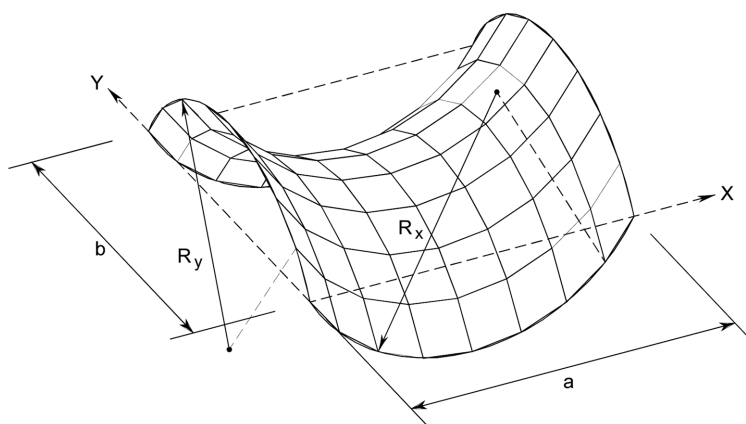


Fig. 5 Hyperbolic paraboloidal shell

Table 2. Non-dimensional fundamental frequencies [$\bar{\omega} = \omega a^2 \sqrt{12\rho(1-v^2)/(Eh^2)}$] of isotropic, corner supported hyperbolic paraboloidal shell

Mode number	This study	ANSYS (Shell 63)	Chakravorty <i>et al.</i> (1995)	Leissa and Narita (1984)
1	17.59	17.71	17.25	17.16
2	38.34	38.92	---	---
3	57.55	59.32	---	---
4	57.55	59.32	---	---
5	77.01	79.83	---	---
6	77.01	79.83	---	---

hyperbolic paraboloidal shell. The geometric parameters are depicted in Fig 5, results obtained are given in Table 2 and compared with Chakravorty *et al.* (1995) and Leissa and Narita (1984).

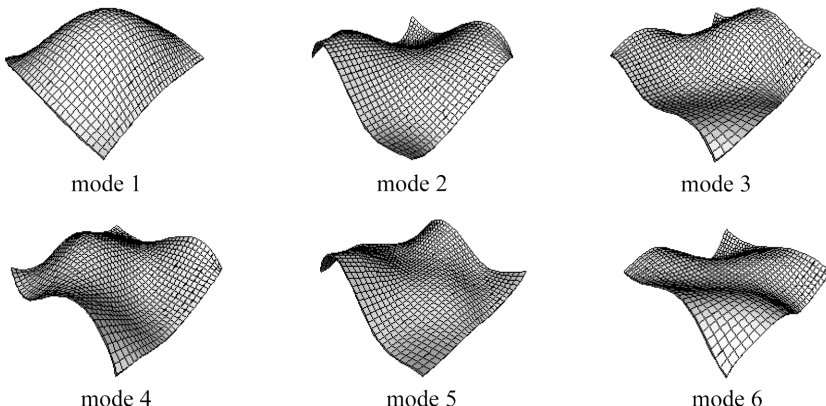


Fig. 6 First six modes of the hypar shell

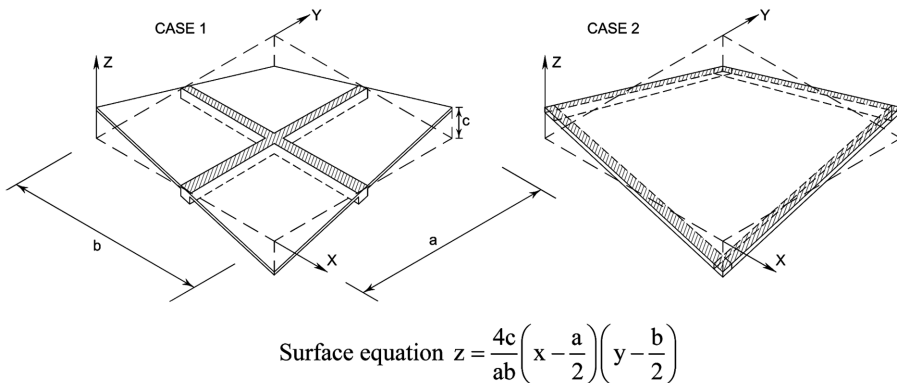


Fig. 7 Hypar shells with stiffeners

The non-dimensional fundamental frequencies are obtained. Results are found to be in good agreement with previous works.

The first six mode shapes of the shell are depicted in Fig.6.

In order to obtain the effect of stiffener location and fiber orientation on vibration behavior of hypar shells two different stiffener locations, different fiber orientations and rise of hypar shell/span ratios (c/a)

Table 3. Non-dimensional fundamental frequencies [$\bar{\omega} = \omega a^2 \sqrt{\rho/(E_1 h^2)}$]

c/a	Case	$\phi = 0^\circ$	$\phi = 30^\circ$	$\phi = 45^\circ$	$\phi = 60^\circ$	$\phi = 90^\circ$
0.025	Case 0	2.493	2.627	2.858	3.291	4.347
0.025	Case 1	2.682	2.862	3.185	3.778	4.885
0.025	Case 2	4.701	4.782	4.930	5.176	5.650
0.05	Case 0	2.770	2.933	3.208	3.708	4.317
0.05	Case 1	2.897	3.094	3.437	4.057	5.273
0.05	Case 2	5.494	5.803	6.131	6.484	6.862
0.10	Case 0	2.938	3.250	3.588	3.960	4.200
0.10	Case 1	3.316	3.557	3.958	4.652	5.902
0.10	Case 2	5.332	5.690	6.037	6.365	6.649
0.20	Case 0	2.666	3.011	3.348	3.678	3.798
0.20	Case 1	3.473	3.751	4.200	4.934	6.074
0.20	Case 2	4.778	5.133	5.456	5.734	5.928
0.25	Case 0	2.498	2.838	3.161	3.464	3.551
0.25	Case 1	3.320	3.591	4.027	4.735	5.792
0.25	Case 2	4.439	4.775	5.075	5.328	5.492
0.30	Case 0	2.325	2.652	2.957	3.233	3.296
0.30	Case 1	3.098	3.354	3.765	4.434	5.416
0.30	Case 2	4.092	4.403	4.680	4.908	5.047

$a = b$, $h/a = 0.012$, $E_1 = 4.667E_2$, $G_{12} = G_{13} = 0.5E_2$, $G_{23} = 0.473E_2$, $\nu_{12} = \nu_{21} = 0.26$, $b_{st}/h = 2$, $d_{st}/h = 4$ (Case 1), $d_{st}/h = 2$ (Case 2).

a) are taken into account. The geometric parameters and stiffener locations are depicted in Fig. 7. Case-0 is bare hypar shell without stiffeners. In Case-1, two perpendicular central stiffeners are placed. In Case-2 stiffeners are placed along the edges by reducing the height to half for keeping the same weight. System is simply supported ($u = v = z = 0$) at four corners.

The non-dimensional circular frequencies ($\bar{\omega}$) are given in Table 3.

The variations of $\bar{\omega}$ given in Table 3. shows that in most cases stiffeners located along the edges increase the fundamental frequency more effectively than two perpendicular central stiffener configuration. Material angle can significantly effect the fundamental frequency.

Conclusions

The development of an element for analysis of hypar shells was presented. The element may successfully solve the vibration problems of stiffened hypar shells and results are in a good agreement with other published studies.

On the basis of the representative numerical examples, the good accuracy of the proposed element for free vibration analysis of hypar shell structures has been demonstrated. The test results show that the element can be effectively be used for such structures.

The present study also gives ideas about the effectiveness of two different stiffener configurations which are mostly used in practice for increasing the fundamental frequency of a bare hypar shell by stiffening. Table 3 combines these possibilities and will help a practicing engineer to choose an optimum solution considering both economy and other practical limitations.

Acknowledgements

The author gratefully acknowledge the excellent support and encouragement provided by Professor Dr. Nahit Kumbasar.

References

- Allman, D. J. (1984), "A compatible triangular element including vertex rotations for plane elasticity problems", *Comp. Struct.*, **19**(1-2), 1-8.
- ANSYS. (1997), Swanson Analysis Systems, Swanson J. ANSYS 5.4. USA.
- Bergan, P. G. and Felippa, C. A. (1985), "A triangular membrane element with rotational degrees of freedom", *Comp. Methods Appl. Mech. Eng.*, **50**(1), 25-69.
- Chakravorty, D., Bandyopadhyay, J.N. and Sinha, P.K. (1995), "Free vibration analysis of point-supported laminated composite doubly curved shells – A finite element approach", *Comp. Struct.*, **54**(2), 191-198.
- Choi, C. K. and Lee, W. H. (1996), "Versatile variable-node flat-shell element", *J. Eng. Mech.*, **122**(5), 432-441.
- Civalek, Ö. (2007), "Linear vibration analysis of isotropic conical shells by discrete singular convolution (DSC)", *Struct. Eng. Mech.*, **25**(1), 127-130.
- Cook, R. D. (1986), "On the Allman triangle and a related quadrilateral element", *Comp. Struct.*, **22**(6), 1065-1067.
- Darilmaz, K. (2005), "An assumed-stress finite element for static and free vibration analysis of Reissner-Mindlin plates", *Struct. Eng. Mech.*, **19**(2), 199-215.
- Darilmaz, K. ,(2005) "A hybrid 8-node hexahedral element for static and free vibration analysis", *Struct. Eng. Mech.*, **21**(5), 571-590.
- Dogan, A. Arslan, H.M. and Yerli, H.R. (2010), "Effects of anisotropy and curvature on free vibration

- characteristics of laminated composite cylindrical shallow shells”, *Struct. Eng. Mech.*, **35**(4), 493-510.
- Das, H.S. and Chakravorty, D. (2010), “A finite element application in the analysis and design of point-supported composite conoidal shell roofs: suggesting selection guidelines”, *The Journal of Strain Analysis for Engineering Design*, **45**(3), 165-177.
- Ibrahimbegovic, A. Taylor, R.L. and Wilson, E.L. (1990), “A robust quadrilateral membrane finite element with drilling degrees of freedom”, *Int. J. Numer. Methods Eng.*, **30**(3), 445-457.
- Feng, W. Hoa, S.V. and Huang, Q. (1997), “Classification of stress modes in assumed stress fields of hybrid finite elements”, *Int. J. Numer. Meth. Eng.*, **40**(23), 4313-4339.
- Haldar, S. (2008). “Free vibration of composite skewed cylindrical shell panel by finite element method”, *J. Sound Vib.*, **311**(1-2), 9-19.
- Han, S.C. Kanok-Nukulchai, W. and Lee, W.H. (2011), “A refined finite element for first-order plate and shell analysis”, *Struct. Eng. Mech.*, **40**(2), 191-213 .
- Leissa, A.W. and Narita, Y. (1984), “Vibrations of corner point supported shallow shells of rectangular planform”, *Earthquake Engng. Struct. Dynam.*, **12**(5), 651-661.
- MacNeal, R.H. and Harder, R.L. (1988), “A refined four-noded membrane element with rotational degrees of freedom”, *Comp. Struct.*, **28**(1), 75-84.
- Mukherjee, A. and Mukhopadhyay, M. (1988), “Finite element free vibration of eccentrically stiffened plates”, *Comp. Struct.*, **30**(6), 1303-1317.
- Nanda, N. and Bandyopadhyay, J.N. (2008), “Nonlinear transient response of laminated composite shells”, *J. Eng. Mech.-ASCE*, **134**(11), 983-990.
- Nayak, A.N. and Bandyopadhyay, J.N. (2002), “On the free vibration of stiffened shallow shells”, *J. Sound Vib.*, **255**(2), 357-382.
- Pian, T.H.H. (1964), “Derivation of element stiffness matrices by assumed stress distributions”, *AIAA J.*, **12**, 1333-1336.
- Pian, T.H.H. and Chen, D.P. (1983), “On the suppression of zero energy deformation modes”. *Int. J. Num. Meth. Eng.*, **19**(12), 1741-1752.
- Punch, E.F. and Atluri, S.N. (1984), “Development and testing of stable, isoparametric curvilinear 2 and 3-D hybrid stress elements”, *Comput. Meth. Appl. Mech. Eng.*, **47**(3), 331-356.
- Sahoo, S. and Chakravorty, D. (2008), “Free vibration characteristics of point supported hypar shells-a finite element approach”, *Advances In Vibration Engineering*, **7**(2), 197-205.
- Sahoo, S. and Chakravorty, D. (2006), “Stiffened composite hypar shell roofs under free vibration:Behaviour and optimization aids”, *J. Sound Vib.*, **295**(1-2), 362-377.
- Sahoo, S. and Chakravorty, D. (2005), “Finite element vibration characteristics of composite hypar shallow shells with various edge supports”, *J. Vib. Control*, **11**(10), 1291-1309.
- Sahoo, S. and Chakravorty, D. (2008), “Bending of composite stiffened hypar shell roofs under point load”, *J. Eng. Mech.-ASCE*, **134**(6), 441-454.
- Sinha, G. and Mukhopadhyay, M. (1994), “Finite element free vibration analysis of stiffened shells”, *J. Sound Vib.*, **171**(4), 529-548.
- Schwarze, J. (1994), “Vibrations of corner point supported rhombic hypar-shells”, *J. Sound Vib.*, **175**(1), 105-114.
- Wang, X.H. and Redekop, D. (2011). “Free vibration analysis of moderately-thick and thick toroidal shells”, *Struct. Eng. Mech.*, **39**(4), 449-463.
- Yunus, S.M. Saigal, S. and Cook, R.D. (1989), “On improved hybrid finite elements with rotational degrees of freedom”, *Int. J. Numer. Meth. Eng.*, **28**(4), 785-800.

Appendix 1:

$$[T] = \begin{bmatrix} 1 & 0 & 0 & 0 & 0 & 0 & 0 & 0 & 0 & 0 & 0 \\ 0 & 1 & 0 & 0 & 0 & 0 & 0 & 0 & 0 & 0 & 0 \\ 0 & 0 & 0 & 1 & 0 & 0 & 0 & 0 & 0 & 0 & 0 \\ 0 & 0 & 0 & 0 & 1 & 0 & 0 & 0 & 0 & 0 & 0 \\ 0 & 0 & 0 & 0 & 0 & 1 & 0 & 0 & 0 & 0 & 0 \\ 0 & 0 & 0 & 0 & 0 & 0 & 1 & 0 & 0 & 0 & 0 \\ 0 & 0 & 0 & 0 & 0 & 0 & 0 & 1 & 0 & 0 & 0 \\ 0 & 0 & 0 & 0 & 0 & 0 & 0 & 0 & 1 & 0 & 0 \\ 0 & 0 & 0 & 0 & 0 & 0 & 0 & 0 & 0 & 1 & 0 \\ \frac{1}{2} & 0 & \frac{(y_1 - y_2)}{8} & \frac{1}{2} & 0 & \frac{(y_2 - y_1)}{8} & 0 & 0 & 0 & 0 & 0 \\ 0 & \frac{1}{2} & \frac{(x_2 - x_1)}{8} & 0 & \frac{1}{2} & \frac{(x_1 - x_2)}{8} & 0 & 0 & 0 & 0 & 0 \\ 0 & 0 & 0 & \frac{1}{2} & 0 & \frac{(y_2 - y_3)}{8} & \frac{1}{2} & 0 & \frac{(y_3 - y_2)}{8} & 0 & 0 \\ 0 & 0 & 0 & 0 & \frac{1}{2} & \frac{(x_3 - x_2)}{8} & 0 & \frac{1}{2} & \frac{(x_2 - x_3)}{8} & 0 & 0 \\ 0 & 0 & 0 & 0 & 0 & 0 & \frac{1}{2} & 0 & \frac{(y_3 - y_4)}{8} & \frac{1}{2} & 0 \\ 0 & 0 & 0 & 0 & 0 & 0 & 0 & \frac{1}{2} & \frac{(x_4 - x_3)}{8} & 0 & \frac{1}{2} \\ \frac{1}{2} & 0 & \frac{(y_1 - y_4)}{8} & 0 & 0 & 0 & 0 & 0 & 0 & \frac{1}{2} & 0 \\ 0 & \frac{1}{2} & \frac{(x_4 - x_1)}{8} & 0 & 0 & 0 & 0 & 0 & 0 & 0 & \frac{1}{2} \end{bmatrix}$$

Appendix 2:

Notation

- b_{st} = stiffener width
 E_1, E_2 = moduli of elasticity along x and y axes of element respectively
 G_{12}, G_{13}, G_{23} = shear moduli of elasticity in x-y, x-z and y-z planes of element
 H = shell thickness
 h_{st} = stiffener height
 L = length of element edge
 M_x, M_y, M_z = bending and twisting moments
 N_x, N_y, N_{xy} = in plane forces
 Q_x, Q_y = shear forces
 R_x, R_y = radius of shell
 x, y, z = element local axis
 X, Y, Z = system global axis
 V = Volume
 ν_{12}, ν_{21} = Poisson ratio

[D]	= differential operator matrix
[E]	= elasticity matrix
[G]	= nodal forces corresponding to assumed stress field
[K]	= stiffness matrix
[N]	= shape functions
[P]	= interpolation matrix for stress
[R]	= inertia matrix
[S]	= compliance matrix
[T]	= transformation matrix
{q}, {̇q}	= displacement and velocity components
{u}	= displacements
{β}	= stress parameters
{σ}	= internal forces
ρ	= mass per unit volume
w	= natural circular frequency
ω	= nondimensional frequency parameter
ϕ	= material angle in an element with reference to x-axis